



Impact of number of sensitizer SILAR cycles on the performance of ZnO based PbS quantum dot-sensitized solar cells

Vikram P. Bhalekar^{1,2,*} , M. B. Rajendra Prasad^{2,3}, and Abhijit T. Supekar²

¹ Department of Physics, Arts, Science and Commerce College, Rahata 423107, India

² Advanced Physics Laboratory, SPPU, Pune 411007, India

³ Department of Physics, National Defence Academy, Khadakwasla, Pune, India

Received: 29 May 2023

Accepted: 6 October 2023

Published online:
4 November 2023

© The Author(s), under exclusive licence to Springer Science+Business Media, LLC, part of Springer Nature, 2023

ABSTRACT

In the current report, we have used ZnO as a photoanode prepared by a simple chemical route. PbS quantum dots (QDs) are loaded in to the porous ZnO photoanode by Successive Ionic Layer Adsorption and Reaction (SILAR) technique at room temperature. The fabricated photoanodes are characterized using X-ray diffractometry, UV–Vis absorption spectrophotometry, and Scanning Electron Microscopy. Further, the photo electrochemical and photovoltaic performance of the photoanode based solar cells is studied. The study highlights the effect of number of SILAR cycles on the performance of the device delivering highest photovoltaic performance of 2.30% for the cell employing a photoanode with 4 SILAR cycles of PbS.

1 Introduction

Quantum dot-sensitized solar cells have attracted considerable interest due to their projected high theoretical efficiency and is competing with (Dye Sensitized Solar Cell) DSSC because of the merits of the sensitizer in terms of light harvesting efficiency and stability as against dyes in DSSC [1–7].

Transparent conducting oxides like TiO₂, ZnO, Nb₂O₅, ZrO₂, SnO₂, have gained more interest in the fabrication of photoanode. TiO₂ has so far proved to be the best photoanode in order to show high performance for DSSC as well as QDSSC [8–13]. Similar to that Zinc Oxide (ZnO), which has a wide bandgap (3.3 eV) and also has suitable band position as against

many QDs to facilitate comfortable electron injection from Quantum Dots (QDs) to ZnO [14, 15]. ZnO by virtue of its high electron mobility, diffusion coefficient, high surface stability [16, 17], low synthesis cost, and optoelectronic properties has attracted interest among researchers in basic as well as applied fields. [18, 19].

In view of the above, ZnO is used as a photoanode material and is fabricated using a simple chemical route. QDs provide the ability to match the solar spectrum because of their tunable absorption spectrum and high stability due to their inorganic character [20–23]. Their properties such as significant dipole moment, high extinction coefficient, and low cost compared to organic dyes [1–3] make them good candidates as a sensitizer in solar cells as against Ruthenium-based

Address correspondence to E-mail: bhalekarvp@gmail.com

dyes which are expensive. Also extinction coefficient and absorption for dyes do not satisfy the requirements of highly efficient solar cells unlike QDs [4–7].

IV–VI semiconductors like PbSe, PbS show multiple exciton generation effects [24, 25]. Of these PbS scores over PbSe in terms of ease of synthesis and has emerged as one of the promising candidates among sensitizers used in QDSSC in their nanocrystalline form. Also, Lead Sulphide (PbS) with a bulk band gap of 0.41 eV and Bohr exciton radius of 18 nm [26] has been reported as an efficient sensitizer absorbing in the infrared region. The PbS QDs are prepared by different techniques and used for sensitization of photoanodes [27–31].

In the present report, adhesive, transparent porous ZnO photoelectrodes of uniform and nearly same thickness are prepared to act as photoanodes in the solar cell fabrication over conducting glass substrate of fluorine-doped tin oxide (FTO). The fabricated photoanodes are characterized for their structural, optical and morphological properties using X-ray diffractometry, UV–Vis absorption spectrophotometry, and Scanning Electron Microscopy.

These films are further sensitized with PbS QDs using different number of SILAR cycles. QDSSC are fabricated making use of these PbS sensitized photoanodes with CuS and polysulphide acting as counter electrode and electrolyte, respectively. The fabricated solar cells are characterized using EIS and JV studies for their performance to evaluate the effect of sensitization using SILAR on photoanodes.

2 Experiment and characterization

2.1 Preparation of viscous ZnO paste

The preparation of paste is essential step in solar cell fabrication because the cracks-free surface morphology of photoanode, good adhesion with the substrate, and interconnectivity of particles are essential for good photoanode. For this work, we have used ZnO nanopowder with an average size of 30 nm. Ethylcellulose (EC), α -Terpineol, and Acetyl Acetone are used to prepare the ZnO paste [32]. For the preparation of slurry, 0.5 g ZnO nanopowder was mixed with a 10 ml of Ethanol and grind for a 15 min. The breaking of the microscopic aggregation of powder is done by grinding the suspension, followed by sonication of the same mixture for 1 h. Ethylcellulose ground in ethanol was

then mixed with the above-prepared ZnO suspension, which is used to improve the viscosity of paste and as a pore-filling agent. Dropwise addition of α -Terpineol as an organic surfactant is done to the above mixture and then the suspension is sonicated for 3 h. In the last stage, four to five drops of acetylacetone were added again, followed by 1 h ultrasonication. The process of ultrasonication is useful against aggregation among nanoparticles and it helps to make the paste homogeneous.

2.2 Preparation of porous ZnO photoelectrodes from ZnO paste

The previously prepared nanocrystalline slurry of ZnO is used to prepare porous photoelectrodes of nearly identical and uniform thickness ($\sim 10 \mu\text{m}$) over FTO coated glass substrates using doctor blade technique [33].

The films are allowed to dry in an incubator maintained at 60 °C for 1 h, then annealed through step heating, i.e., at 100, 200, 300 °C each for 15 min and finally at 450 °C for 1 h in order to remove the binder and other organic impurity added during the paste preparation. Besides, annealing also provides good crystallographic arrangement of ZnO particles.

2.3 PbS sensitization of ZnO photoelectrode

The ZnO photoelectrodes as prepared above are sensitized with PbS QDs employing SILAR technique at room temperature. In brief, we have prepared $\text{Pb}(\text{NO}_3)_2$ and Na_2S solutions in double distilled water and ethanol, respectively, with a concentration of 0.02 M for each. Initially, ZnO photoelectrode is immersed in a $\text{Pb}(\text{NO}_3)_2$ aqueous solution for 60 s followed by rinsing in DDW for 30 s. After the adsorption of cations (Pb^{2+}), the reaction with anions (S^{2-}) is done by immersion of photoelectrode in ethanolic solution of Na_2S for 60 s. Finally, the deposited film is again rinsed in DDW for 30 s; it completes one SILAR cycle. Many such SILAR cycles are carried out to prepare photoelectrode samples sensitized with 2, 4, 6, and 8 SILAR cycles respectively. 2, 4, 6, and 8 are referred to as electrode samples subjected to 2, 4, 6, and 8 SILAR cycles, respectively, and accordingly the cells based on 2, 4, 6, and 8 are named 2c, 4c, 6c, and 8c. Surface passivation of PbS QDs deposited over all the film samples is carried out using Cu-ZnS as reported by Jia et al. [34].

2.4 Preparation of electrolyte

Polysulphide electrolyte is prepared by using 0.5 M Sodium Sulphide (Na_2S) and 0.1 M Sulphur powder (S) [35] and used as electrolyte in the solar cells. In brief, Sodium Sulphide and Sulphur powder are taken and ground separately in ethanol, then by mixing them properly with the addition of 2 ml distilled water and 2 ml ethanol resulting in polySulphide electrolyte ready to use for performance measurement.

2.5 Preparation of counter electrode

In the present research, the CuS is used as counter electrode and is prepared by an inexpensive and simple technique [36]. Initially, CuS powder was prepared by using Copper Sulphate (CuSO_4) as a copper source and Sodium Thiosulphate ($\text{Na}_2\text{S}_2\text{O}_3$) as a Sulphur source by taking 0.5 M solution of each with volumetric ratio 1:3. Preparation of paste is done by mixing prepared CuS powder, ethylcellulose with 2-(2-butoxyethoxy) ethyl acetate (20%) as a binder, acetylacetone and ethanol. All the constituents are mixed till a sticky paste is formed. Finally, prepared CuS paste is coated on FTO using a doctor blade technique followed by annealing at 500 °C for 1 h.

3 Results and discussion

3.1 Structural and optical properties

Figure 1a shows the XRD pattern of PbS sensitized ZnO films for 2, 4, 6 & 8 SILAR cycles of PbS. The

X-ray diffractograms shown here represent peaks corresponding to both the materials. It is observed that the diffraction intensities of P(116), P(100) P(202), and P($2\bar{2}6$) representing PbS have gradually shown increment with increase in the number of SILAR cycles inferring the growth of PbS nanocrystal over the porous ZnO electrode of nearly identical thickness. In the combinations of two sets of patterns: one of them is assigned to hexagonal ZnO (JCPDS card No. 36-1451) and another to PbS (JCPDS card No. 05-0592). Thus the XRD results validate the sensitization of PbS over ZnO surface. The peaks of FTO, ZnO, and PbS are highlighted by legends #, Z and P, respectively. The average crystallite size of ZnO nanocrystallites is estimated using Scherer formula and is approximately 56 nm.

Figure 1b depicts the optical spectra band gap and of ZnO/PbS films for 2, 4, 6, and 8 SILAR cycles. A sharp enhancement in the absorption spectra at lower wavelength (below 350 nm) is observed, which corresponds to ZnO, suggesting that its absorption band edge facilitates its application as a wide bandgap semiconductor material. It is also observed that the absorption edge shifts towards the higher wavelength (red-shift) with an increase in a number of SILAR cycles for PbS over ZnO. This result demonstrates that the ZnO film sensitized with PbS absorbs not only the visible region of the solar spectrum but also it extended to the near-infrared region. Increase in absorbance of light in the visible region is observed with increase of number of SILAR cycles from 2 to 8. It also infers that the loading amount of PbS has increased with increasing number of SILAR cycles.

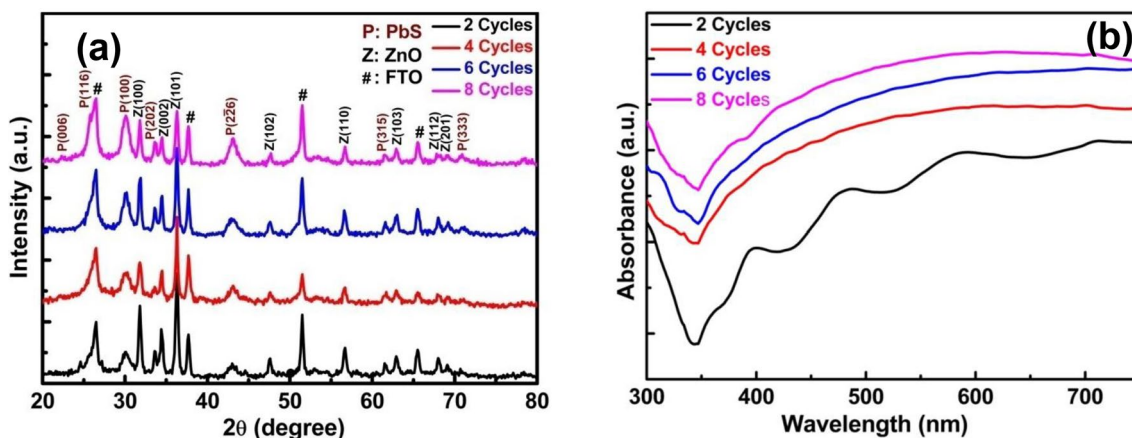


Fig. 1 a XRD pattern b Optical absorbance vs. Wavelength graph of PbS sensitized ZnO films for 2, 4, 6, and 8 SILAR Cycles

3.2 Morphological properties

The surface morphology of ZnO coated with 2, 4, 6, and 8 SILAR cycles of PbS quantum dots is examined using scanning electron microscopy. Figure 2a clearly shows that the photoelectrode is porous and hence facilitated the deposition of PbS nanocrystal. It may be observed from Fig. 2a–d, the porosity of the photoelectrodes has apparently reduced with increased number of SILAR cycles probably due to the increased deposition of PbS nanocrystals covering the pores in the electrode. This is in agreement with the results obtained from optical absorption spectra, which showed enhanced absorbance with the increased PbS QD loading into the electrode. The Fig. 2a–d clearly shows red shift in the absorption edge with increased number of SILAR cycles probably indicating increase in the size of QDs.

3.3 Electrochemical impedance spectra (EIS)

The electrochemical measurement of the ZnO/PbS/Cu-ZnS devices for various PbS SILAR cycles is carried out by impedance spectroscopy. Nyquist plot is shown in Fig. 3b, it shows Warburg like behaviour in the frequency transition region from high frequency to intermediate frequency [37]. It is inferred that greater the slope of linear portion in this region smaller is the electron transport resistance (R_t) in the electrode. It may be observed from the plot that the R_t is nearly same for the samples 4 and 2 cycles followed by relatively greater R_t for 6 and 8 cycles. The bode phase plots in the Fig. 3c shows the electron life times at the ZnO/PbS/Cu-ZnS/ electrolyte for the electrodes samples increase in the order 8, 6, 2, and 4 cycles. The electron lifetimes calculated from the plots is tabulated in Table 1.

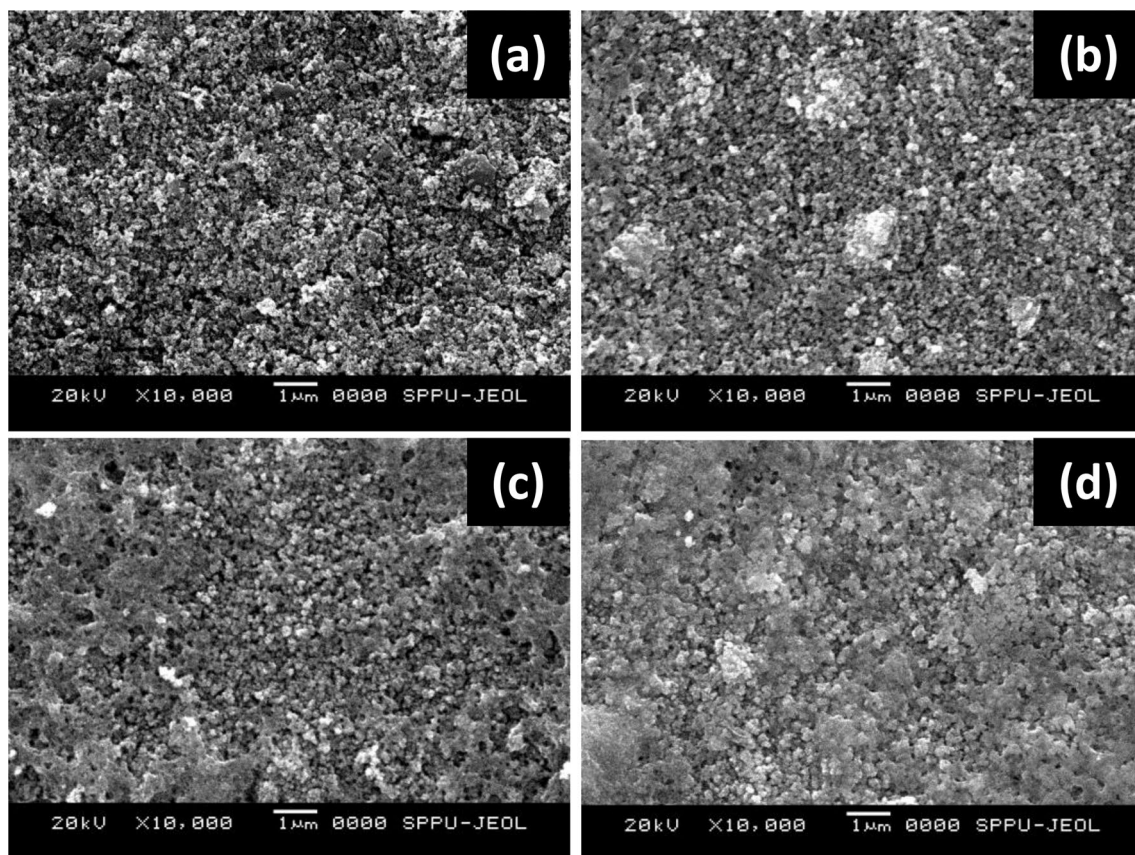


Fig. 2 SEM images of PbS sensitized ZnO films for **a** 2 **b** 4 **c** 6, and **d** 8 SILAR Cycles

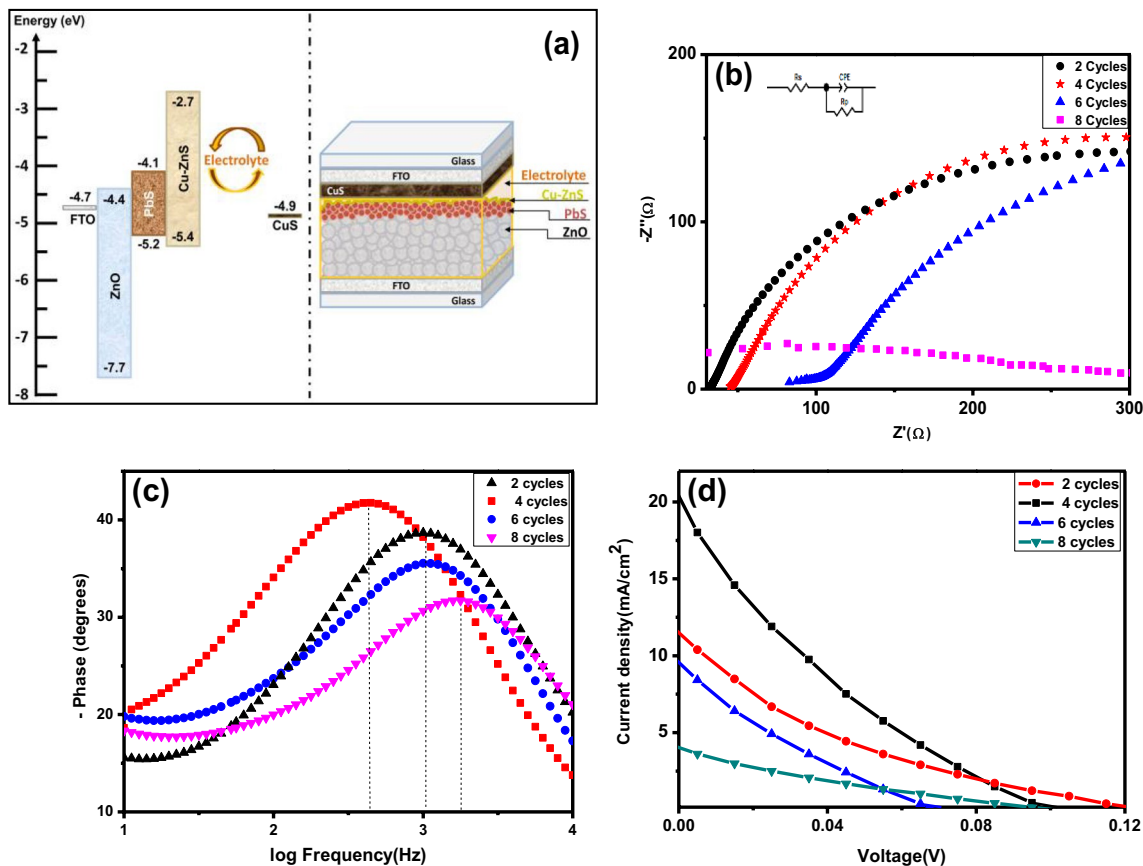


Fig. 3 **a** Schematic diagram of complete ZnO/PbS/Cu–ZnS based device along with energy level diagram. The values of energies were taken from the reference [32–35]. **b** Nyquist plots

with equivalent circuit (inset), **c** Bode phase plots and **d** J–V curve for ZnO/PbS/Cu–ZnS films at various PbS SILAR Cycles

Table 1 The electron lifetimes PbS sensitized solar cells for different SILAR cycles

Sr. no.	Sample no.	Life time (τ_c) ms
1	2c	0.16
2	4c	0.35
3	6c	0.16
4	8c	0.09

It means the recombination resistance are maximum for 4 and minimum for sample of 8 cycles. The relation between charge collection efficiency η_{cc} , R_t , R_r , and L (thickness) may be given by Eq. (1) [37–41].

$$\eta_{cc} = 1 - \left(\frac{R_t}{R_r}\right) L^2 \tag{1}$$

However, for the present set of samples the thickness of all electrodes being nearly the same, η_{cc} (Charge

Collection efficiency) only depends on R_t/R_r . From the aforesaid discussion on Nyquist and Bode phase plot qualitatively R_t/R_r is minimum for ‘4c’ and maximum for 8c inferring maximum charge collection for 4c and minimum 8c.

3.4 J–V characteristics

Figure 3a depicts the energy band alignment schematic diagram of the complete ZnO/PbS/Cu–ZnS/electrolyte/CuS counter electrode device. The photocurrent density–voltage (J–V) curves of ZnO/PbS/Cu–ZnS solar cells for 2–8 PbS SILAR cycles are shown in Fig. 3d. The photovoltaic output parameters include short-circuit current density (J_{sc}), open-circuit voltage (V_{oc}), fill factor (FF), and efficiency (η). The device with 4 PbS SILAR cycles shows superior performance (2.30%) than the rest of the devices. The current density of a solar cell depends on external quantum efficiency which in turn depends on electron

Table 2 Photovoltaic output parameters of fabricated PbS sensitized solar cells for different SILAR cycles of PbS

Samples	2c	4c	6c	8c
V_{oc} (mV)	125	98	68	100
J_{sc} (mA/cm ²)	11.50	20.39	9.57	4.03
Fill Factor (%)	14.0	17.0	19.0	18.0
Efficiency (%)	1.34 ± 0.20	2.3 ± 0.1	0.85 ± 0.17	0.5 ± 0.1

transfer yield that is decided by the charge collection efficiency. In other words, the current density implicitly depends on the charge collection efficiency. This is evident from the J–V characteristics, Fig. 3d of the solar cells assembled from the films 2, 4, 6, and 8 namely 2c, 4c, 6c, and 8c. It is observed that the efficiency of the QDSSC is driven by J_{sc} . This inference is justified since photovoltaic efficiencies obtained for these cells exactly followed the same trend as that of J_{sc} as shown in the Table 2. It may be observed that, J_{sc} being driven by n_{cc} is affected by number of SILAR cycles on the ZnO electrode surface. To elaborate, the QDs deposited through SILAR cycles gradually cover the entire electrode surface with increase of number of SILAR cycles probably giving optimal coverage for 4 cycles. This may have probably bestowed the sample with maximum R_r and minimum R_t in conformity with the EIS studies discussed above, leading to enhanced charge collection efficiency and hence maximum current density (20.39 mA/cm²) in respect of '4c'. From the efficiency trends or the trends of J_{sc} it may be inferred that for 2c the coverage of QDs is insufficient thus showing relatively less recombination resistance at the ZnO/electrolyte interface. However, for 6 and 8 the QD coverage is over and above leading to aggregation of PbS nanocrystals leading to enhanced electron–hole recombination and hence reduced current densities finally affecting the cell performance.

4 Conclusion

In the present work, ZnO/PbS QDs solar cells are assembled with CuS as the counter electrode and polysulphide as the electrolyte. The impact of QD sensitization over the electrode surface by increasing the number of SILAR cycles is studied. It has been observed that maximum performance of 2.30%

is obtained for the solar cell containing electrode with 4 SILAR cycle QD deposition. This is probably one of the best performances of a PbS sensitized ZnO solar cells ever reported with counter electrode and electrolyte systems used here. It has been observed that the QD coverage driven by the number of SILAR cycles has significantly influenced the current density of the solar cells and hence proved pivotal in deciding the photovoltaic performance of the QDSSC. It has been observed that neither undercoverage nor overcoverage of QDs on the photoelectrodes has proved beneficial in the improvement of photovoltaic efficiency. The conformal coating of QDs over ZnO yielded maximum photo conversion efficiency as is the case with '4c' emphasizing on significance of the number of SILAR cycles to obtain better performance in such solar cell architectures.

Acknowledgements

Authors are thankful to University with Potential for Excellence (UPE)–II, University Grants Commission, New Delhi, India for financial support.

Author contributions

VPB: Data curation, concepts, writing—review and editing. MBRP: Conceptualization, review and editing. ATS: Data curation, review.

Funding

No funding is available for the research to any author.

Data availability

The raw/processed data required to reproduce these findings cannot be shared at this time as the data also forms part of an ongoing study.

Declarations

Conflict of interest The authors declare that they have no conflict of interest.

References

- C.J. Raj, S.N. Karthick, S. Park, K.V. Hemalatha, S.K. Kim, K. Prabakar, H.J. Kim, Improved photovoltaic performance of CdSe/CdS/PbS quantum dot sensitized ZnO nanorod array solar cell. *J. Power. Sources* **248**, 439–446 (2014)
- P.R. Nikam, P.K. Baviskar, J.V. Sali, K.V. Gurav, J.H. Kim, B.R. Sankapal, CdS surface encapsulated ZnO nanorods: synthesis to solar cell application. *J. Alloy. Compd.* **689**, 394–400 (2016)
- A.J. Nozik, M.C. Beard, J.M. Luther, M. Law, R.J. Ellingson, J.C. Johnson, Semiconductor quantum dots and quantum dot arrays and applications of multiple exciton generation to third-generation photovoltaic solar cells. *Chem. Rev.* **110**, 6873–6890 (2010)
- D. Karageorgopoulos, E. Stathatos, E. Vitoratos, Thin ZnO nanocrystalline films for efficient quasi-solid state electrolyte quantum dot sensitized solar cells. *J. Power. Sources* **219**, 9–15 (2012)
- J. Yang, A. Sharma et al., Structurally driven ultrafast charge funneling in organic bulk heterojunction hole transport layer for efficient colloidal quantum dot photovoltaics. *Adv. Mater.* **13**(20), 2203749 (2023)
- A.R. Kirmani, A.D. Sheikh et al., Overcoming the ambient manufacturability-scalability-performance bottleneck in colloidal quantum dot photovoltaics. *Adv. Mater.* **30**(35), 1801661 (2018)
- R. Wang, Wu. Xun et al., Highly efficient inverted structural quantum dot solar cells. *Adv. Mater.* **30**(15), 1704882 (2018)
- J. Tian, R. Gao, Q. Zhang, S. Zhang, Y. Li, J. Lan, X. Qu, G. Cao, Enhanced performance of CdS/CdSe quantum dot co-sensitized solar cells via homogeneous distribution of quantum dots in TiO₂ film. *J. Phys. Chem. C* **116**, 18655–18662 (2012)
- J. Plain, M. Tréguer-Delapierre, Structural analysis and characterization of lead oxide. *Exp. Theor. Nanotechnol.* **6**(4), 453–472 (2022)
- G. Arora, I. Hiroya, Annealing temperature effect on structural properties of tin oxide nanoparticles. *Exp. Theor. Nanotechnol.* **6**(1), 39–46 (2022)
- Y. Al-Douri, H. Khachai, R. Khenata, A. Bouhemadou, First-principles calculations for optical investigations of Pb_x (X = S, Te) compounds under quantum dots diameter effect. *Can. J. Phys.* **93**, 1490–1494 (2015)
- Y. Al-Douri, H. Khachai, R. Khenata, Chalcogenides-based quantum dots: optical investigation using first-principles calculations. *Mater. Sci. Semiconductor Process.* **39**, 276–282 (2015)
- V.P. Bhalekar, ‘Quantum dots sensitized solar cell’, quantum dots—recent advances, new perspective and contemporary application. IntechOpen (2023). <https://doi.org/10.5772/intechopen.107266>
- L. Peng, H. Hong, Y. Shi, X. Zhou, Y. Lin, J. Jia, High performance CdSe quantum dot sensitized ZnO solar cell fabricated from ion exchange. *J. Alloy. Compd.* **765**, 355–361 (2018)
- F. Lu, W. Cai, Y. Zhang, ZnO hierarchical micro/nanoarchitectures: solvothermal synthesis and structurally enhanced photocatalytic performance. *Adv. Funct. Mater. Funct. Mater.* **18**, 1047–1056 (2008)
- M. Quintana, T. Edvinsson, A. Hagfeldt, G. Boschloo, Comparison of dye-sensitized ZnO and TiO₂ solar cells: studies of charge transport and carrier lifetime. *J. Phys. Chem. C* **111**, 1035–1041 (2007)
- D.C. Look, D.C. Reynolds, J.R. Sizelove, R.L. Jones, C.W. Litton, G. Cantwell, W.C. Harsch, Electrical properties of bulk ZnO. *Solid State Commun. Commun.* **105**, 399–401 (1998)
- P. Tiwana, P. Docampo, M.B. Johnston, H.J. Snaith, L.M. Herz, Electron mobility and injection dynamics in mesoporous ZnO, SnO₂, and TiO₂ films used in dye-sensitized solar cells. *ACS Nano* **5**(6), 5158–5166 (2011)
- W.W. Yu, L. Qu, W. Guo, X. Peng, Experimental determination of the extinction coefficient of CdTe, CdSe, and CdS nanocrystals. *Chem. Mater.* **15**(14), 2854–2860 (2003)
- P. Wang, S.M. Zakeeruddin, J.E. Moser, R. Humphry-Baker, P. Comte, V. Aranyos, A. Hagfeldt, M.K. Nazeeruddin, M. Grätzel, Stable new sensitizer with improved light harvesting for nanocrystalline dye-sensitized solar cells. *Adv. Mater.* **16**(20), 1806–1811 (2004)
- R. Vogel, P. Hoyer, H. Weller, Quantum-sized PbS, CdS, Ag₂S, Sb₂S₃, and Bi₂S₃ particles as sensitizers for various nanoporous wide-bandgap semiconductors. *J. Phys. Chem.* **98**(12), 3183–3188 (1994)
- R. Vogel, K. Pohl, H. Weller, Sensitization of highly porous, polycrystalline TiO₂ electrodes by quantum sized CdS. *Chem. Phys. Lett.* **174**(3–4), 241–246 (1990)
- B.Q. Shen, K. Katayama, T. Sawada, S. Hachiya, T. Toyoda, Ultrafast carrier dynamics in PbS quantum dots. *Chem. Phys. Lett.* **542**, 89–93 (2012)
- D. Vankhade, A. Kothari, T.K. Chaudhuri, Direct-coated photoconducting nanocrystalline PbS thin films with tunable band gap. *J. Electron. Mater.* **45**, 2789–2795 (2016)
- V.P. Bhalekar et al., Lead sulphide sensitized ZrO₂ photoanode for solar cell application with MoO₃ as a counter electrode. *Chem. Phys. Lett.* **689**, 15–18 (2017)
- E.H. Sargent, Colloidal quantum dot solar cells. *Nat. Photonics* **6**, 133–135 (2012)

27. A.H. Ip, S.M. Thon, S.H. Hoogland, O. Voznyy, D. Zhitomirsky, R. Debnath, L. Levina, L.R. Rollny, G.H. Carey, A. Fischer, K.W. Kemp, I.J. Kramer, Z. Ning, A.J. Labelle, K.W. Chou, A. Amassian, E.H. Sargent, Hybrid passivated colloidal quantum dot solids. *Nat. Nanotechnol.* **7**, 577–582 (2012)
28. K. Zhao, Z. Pan, I. Mora-Seró, E. Cánovas, H. Wang, Y. Song, X. Gong, J. Wang, M. Bonn, J. Bisquert, X. Zhong, Boosting power conversion efficiencies of quantum-dot-sensitized solar cells beyond 8% by recombination control. *J. Am. Chem. Soc.* **137**(16), 5602–5609 (2015)
29. M.B.R. Prasad, J.T. Abraham, C. Rajesh et al., An ultrasonication based facile protocol to synthesize mesoporous nanocrystalline TiO₂ as photo anode for application in quantum dot/perovskite sensitized solar cell. *J. Electron. Mater.* **48**, 3183–3193 (2019)
30. V.P. Bhalekar, H.M. Pathan, Strong quantum confined lead sulphide quantum dots using ionic reaction and their properties. *ES Mater. Manuf.* **3**, 52–56 (2019)
31. V.P. Bhalekar et al., PbS sensitized TiO₂ based quantum dot solar cells with efficiency greater than 5% under artificial light: effect of compact layer and surface passivation. *Eng. Sci.* **7**, 38–42 (2019)
32. S.K. Dhungel, J.G. Park, Optimization of paste formulation for TiO₂ nanoparticles with wide range of size distribution for its application in dye sensitized solar cells. *Renew. Energy* **35**(12), 2776–2780 (2010)
33. H.K. Jun, M.A. Careem, A.K. Arof, Fabrication, characterization, and optimization of CdS and CdSe quantum dot-sensitized solar cells with quantum dots prepared by successive ionic layer adsorption and reaction. *Int. J. Photoenergy* **2014**, 939423 (2014). <https://doi.org/10.1155/2014/939423>
34. J. Jia, C. Liu, Y. Lin, X. Zhou, Large enhancement in cell performance of CdSe-sensitized ZnO solar cell via ZnSe overcoating. *J. Alloy. Compd.* **727**, 80–85 (2017)
35. M.B. Rajendra Prasad et al., Impact of composition of polysulphide electrolyte on the photovoltaic performance in quantum dot sensitized solar cells. *Mater. Res. Express* **5**, 066208 (2018)
36. B.M. Palve, V.S. Kadam, C.V. Jagtap, S.R. Jadkar, H.M. Pathan, A simple chemical route to synthesis the CuSe and CuS counter electrodes for titanium oxide-based quantum dot solar cells. *J. Mater. Sci. Mater. Electron.* **28**, 14394–14401 (2017)
37. S.R. Gajjela, C. Yap, P. Balaya, Multi-functional photoanode films using mesoporous TiO₂ aggregate structure for efficient dye sensitized solar cells. *J. Mater. Chem.* **22**(21), 10873–10882 (2012)
38. Y. Tachibana, K. Hara, K. Sayama, H. Arakawa, Quantitative analysis of light-harvesting efficiency and electron-transfer yield in ruthenium-dye-sensitized nanocrystalline TiO₂ solar cells. *Chem. Mater.* **14**(6), 2527–2535 (2002)
39. K. Tvrđy, P.A. Frantsuzov, P.V. Kamat, Photoinduced electron transfer from semiconductor quantum dots to metal oxide nanoparticles. *Proc. Natl. Acad. Sci.* **108**(1), 29–34 (2011)
40. Y.L. Lee, Y.S. Lo, Highly efficient quantum-dot-sensitized solar cell based on co-sensitization of CdS/CdSe. *Adv. Func. Mater.* **19**(4), 604–609 (2009)
41. R.S. Dibbell, D.F. Watson, Distance-dependent electron transfers in tethered assemblies of CdS quantum dots and TiO₂ nanoparticles. *J. Phys. Chem. C* **113**(8), 3139–3149 (2009)

Publisher's Note Springer Nature remains neutral with regard to jurisdictional claims in published maps and institutional affiliations.

Springer Nature or its licensor (e.g. a society or other partner) holds exclusive rights to this article under a publishing agreement with the author(s) or other rightsholder(s); author self-archiving of the accepted manuscript version of this article is solely governed by the terms of such publishing agreement and applicable law.